AJNR

Dynamic 3D MR Angiography of Intra- and Extracranial Vascular Malformations at 3T: A Technical Note

S. Ziyeh, R. Strecker, A. Berlis, J. Weber, J. Klisch and I. Mader

AJNR Am J Neuroradiol 2005, 26 (3) 630-634
http://www.ajnr.org/content/26/3/630

AJNR Am J Neuroradiol 26:630–634, March 2005

Technical Note

Dynamic 3D MR Angiography of Intra- and Extracranial Vascular Malformations at 3T: A Technical Note

S. Ziyeh, R. Strecker, A. Berlis, J. Weber, J. Klisch, and I. Mader

Summary: Time-resolved, contrast-enhanced 3D MR angiography combined with parallel imaging at 3T was applied to an intracranial arteriovenous malformation, a dural arteriovenous fistula, and an extracranial facial arteriovenous malformation. The temporal resolution was one image every 1.5 seconds. Arterial feeders were depicted in all three cases. Early venous drainage was observed in the intracerebral arteriovenous malformation and the dural arteriovenous fistula, but not in the facial arteriovenous malformation. All findings were concordant with conventional angiography.

Spatial resolution of contrast-enhanced 2D projection MR angiography (MRA) is restricted when a temporal resolution of two frames per second is obtained (1–3). This technique has special advantages for MR imaging of vascular malformations, because the hemodynamics of the pathologic process can be assessed (4–9). Contrast-enhanced 3D MRA can achieve a better spatial resolution at the cost of temporal resolution. Parallel imaging techniques allow an additional reduction of acquisition time and, hence, an improvement of temporal resolution at preserved spatial resolution (10, 11). An advance for dynamic 3D contrast-enhanced MRA may derive from a higher magnetic field with increased signal intensity from blood and a better saturation of the brain tissue in the background. Thus, we combined dynamic contrast-enhanced 3D MRA at 3T with parallel imaging to evaluate these techniques in view of the efficacy of its temporal resolution of an intracranial arteriovenous malformation (iAVM), a dural arteriovenous fistula (dAVF), and an extracranial facial arteriovenous malformation (eAVM). A comparison with conventional catheter digital subtraction angiography (DSA) was performed.

Received July 14, 2004; accepted after revision September 14.

From the Neurocenter, Section of Neuroradiology (S.Z., A.B., J.W., J.K., I.M.), and the MR Development and Application Center, Dept. of Diagnostic Radiology (R.S.), Freiburg University Hospital, Freiburg, Germany.

Address correspondence to PD Dr. med. Irina Mader, Neurocenter, Section of Neuroradiology, Freiburg University Hospital, Breisacher Strasse 64, D-79106 Freiburg, Germany.

Description of Techniques

All MR imaging measurements were performed on a 3T whole-body system by using an eight-element phased-array head coil. Dynamic MRA was performed by using a 3D fast low-angle shot (FLASH) sequence (12) with the following parameters: TE/TR, 1.62/4.31 ms; bandwidth, 490 Hz/Px; partially sampling a k-space volume of 256 × 256 × 16 data points, with an in-plane image resolution of 0.8 × 0.8 mm and a section resolution of 6 mm. Parallel imaging with a GRAPPA factor (*gener*alized *a*utocalibrating *p*artially *p*arallel *a*cquisitions) of two was applied in phase-encoding direction sampling of 24 reference lines in the k-space center (13). This technique allows the acquisition of one 3D data set with the described sequence parameters in 1.5 seconds. The measurements were repeated 22 (dAVF and eAVM) and 25 times (iAVM). Contrast injection was started 7 seconds after start of measurement. To eliminate background nonvascular signal intensity, a mean mask from the first four data sets was calculated and image subtraction of the dynamic data sets from the precontrast mask was performed. Further processing and image evaluation was then done on the subtraction images. A standard dose of 0.1 mmol/kg body weight gadolinium-gandobenate dimeglumine (Multihance, Altana, Konstanz, Germany) followed by 20 mL of physiologic saline solution was applied via the cubital vein. Because no injection system for a 3T unit was commercially available at this time, a manual injection of about 2 mL/s was performed.

Applications

iAVM

The diagnosis of a high-flow iAVM in the left central region was primarily established by MR imaging and a selective, conventional DSA in a 56-year-old patient presenting with headache and a suspected motor Jacksonian seizure. A partial embolization of the iAVM using Ethibloc had been performed 2 months earlier.

dAVF

The diagnosis of a bilateral dAVF emerging from anterior ethmoidal arteries (dural branches of the ophthalmic arteries) was established by conventional catheter DSA in a 51-year old patient with a pulse synchronous tinnitus. A first embolization of the right side with histoacryl had been performed before.

eAVM

The diagnosis of an eAVM in the region of the right mandible was primarily established by MR imaging and a selective, conventional DSA in this 39-year old patient. A partial embolization of two feeding arteries by using Ethibloc had been performed two months before.

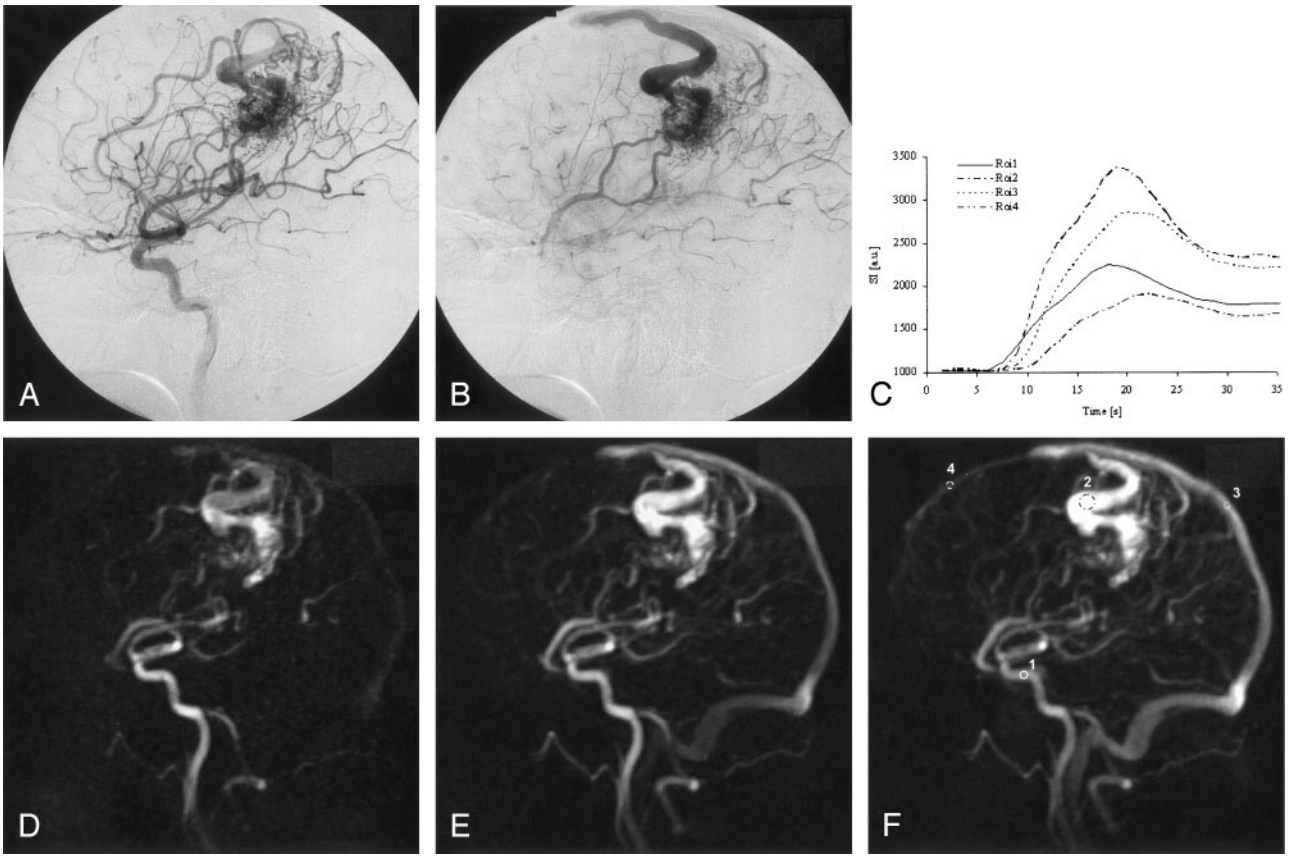

FIG 1. Conventional catheter DSA (*A, B*) reveals a high-flow AVM with a left central nidus fed by a central branch of the middle cerebral artery and an enlarged callosomarginal artery. A superficial and cortical vein is draining into the frontoparietal superior sagittal sinus. The time difference between *A* and *B* is 0.5 seconds.

The dynamic MRA (*D, E*) depicts both the arterial feeders and the drainage vein. The nidus itself is poorly depicted and superposed by the early filled enlarged cortical vein. A region-of-interest analysis of the time signal intensity course (*C, F*) was performed within the internal carotid artery (region 1), the drainage vein (region 2), the parietal superior sagittal sinus (region 3), which was fed by the drainage vein, and the frontal superior sagittal sinus (region 4), showing anterograde flow and no blood supply from the iAVM as established by conventional DSA. The time course of the signal intensity within the region of interest is given in arbitrary units. The difference of contrast arrival time between the internal carotid artery (region 1) and the dominant drainage vein (region 2) was 2 seconds. The difference of time to peak was 1 second, whereas the difference of contrast arrival time between the internal carotid artery and the normally fed frontal superior sagittal sinus was 4 seconds, and the difference of time to peak was 3 seconds. This reflects the flow pattern of the high-flow AVM, where the venous drainage system is already filled in the early arterial perfusion phase. The regular time of the venous perfusion phase is shown by the time course of the frontal sagittal superior sinus, and is in the normal range (4–7 seconds) as given by Noguchi et al (7).

All three patients received dynamic MRA before endovascular intervention, because the routine protocol includes an MR investigation with time-resolved MRA before further endovascular treatment. Catheter DSA was performed, and those series were taken into account for comparison, where the catheter was placed in the internal carotid artery (iAVM and dAVF), and external carotid artery (eAVM), respectively.

Discussion

Dynamic 2D MR projection angiography was primarily described by Wang et al (1) and modified by Hennig et al (2), reaching a temporal resolution in the subsecond domain. One of the major drawbacks of these time-resolved methods is the low signal intensity-to-noise ratio due to the fast acquisition time. Processing strategies derived from functional imaging as correlation analysis can be applied, leading to an increase of the signal intensity-to-noise ratio and a reduction of background noise (3). Cerebral dural arteriovenous fistulas (5–7), intracranial vascular malformations (4, 8), and extracranial vascular malformations (9) have been investigated by using contrast-enhanced 2D projection techniques. Meanwhile, time-resolved techniques give a better temporal resolution by using modified methods of k-space filling, and 3D acquisitions can be obtained at a higher spatial resolution. Coley et al (14) reached a temporal resolution of one frame per second by using a radial-projection sliding window technique. Time-resolved contrast-enhanced 3D MRA of the whole brain could be performed at a temporal resolution of one frame per 1.8–2.1 second by using parallel imaging at 1.5T (15).

In this technical note, dynamic contrast-enhanced 3D MRA at 3T combined with parallel imaging was

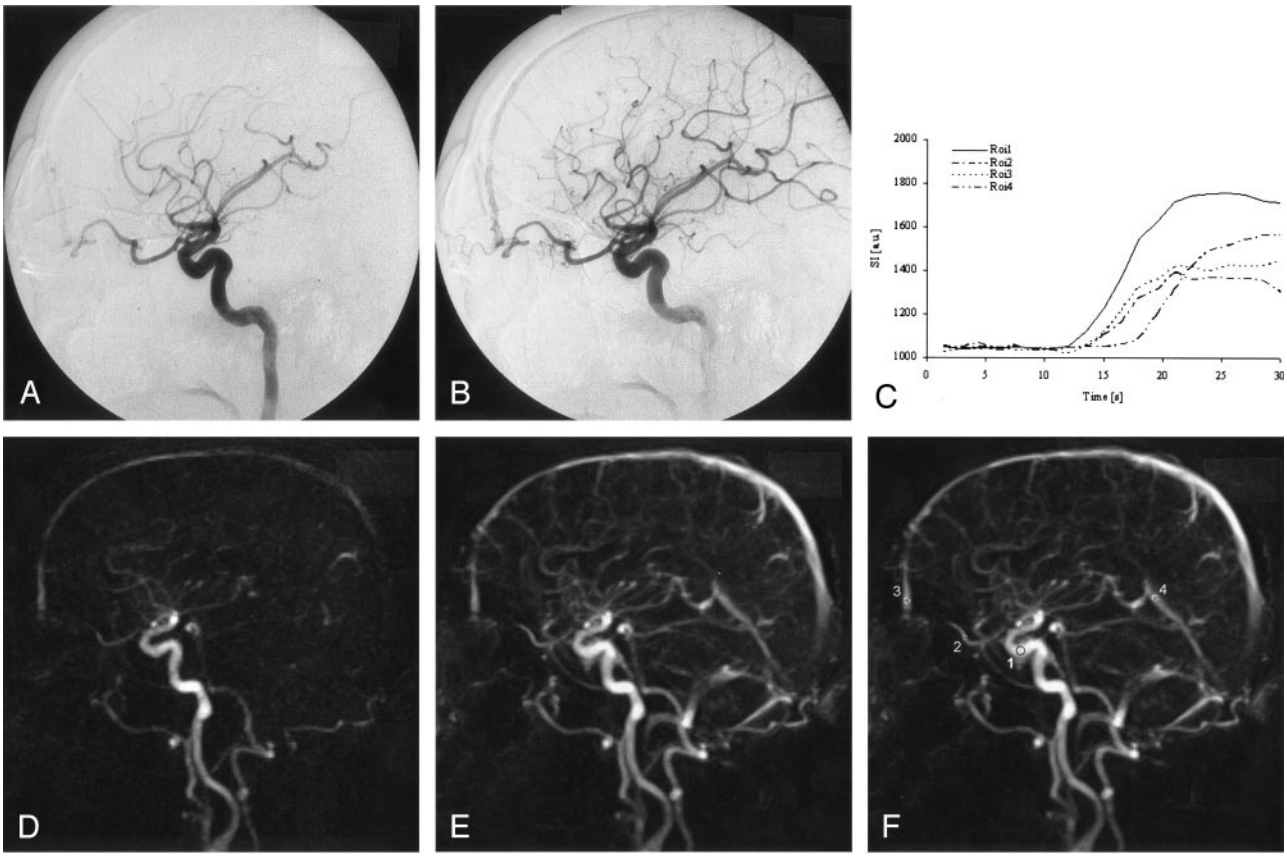

FIG 2. Conventional catheter DSA (*A, B*) obtained at two frames per second shows an enlarged ophthalmic artery feeding a dural arteriovenous fistula. The anterior ethmoidal artery is the supplying arterial feeder. The fistula point is in the midline at the dural passage. The frontal sagittal superior sinus is immediately filled during the early arterial phase.

Dynamic 3D MRA (*D, E*) depicted the residual dAVF arising from the ophthalmic artery and a filling of the frontal superior sagittal sinus during the very early arterial phase. The direct point of the fistula can only be suspected, whereas the supplying arteries and their hemodynamics can be observed. A region-of-interest analysis of the signal intensity time course (*C, F*) was performed within the internal carotid artery (region 1), the ophthalmic artery (region 2), the superior sagittal sinus (region 3), which was fed by the drainage vein, and the sinus rectus (region 4), which was not supplied by blood from the dAVF. The time course of the SI within the region of interest is given in arbitrary units. The differences of the dynamics of contrast enhancement between the internal carotid artery, the ophthalmic artery and the superior sagittal sinus were below the temporal resolution of our sequence. This reflects the very fast hemodynamics of the high-flow dAVF, where the venous drainage system is nearly simultaneously filled with the early arterial perfusion phase. This finding was confirmed by conventional angiography, where arterial and venous contrast appearance was also simultaneous.

performed by taking advantage of the reduction of acquisition time established by parallel imaging and the higher signal intensity-to-noise ratio at 3T. A temporal resolution of one 3D data set every 1.5 seconds could be achieved by using a parallel imaging technique. The expected improvement of the signal intensity at 3T in combination with the saturation effects onto the stationary background tissue (due to the prolonged T1 relaxation times at 3T) was additionally advantageous.

The temporal resolution was sufficient for the extracranial and intracranial AVM. In the high-flow iAVM an arteriovenous transit time of 1 second could be detected. A normal transit time of 3 seconds in this case could be established in healthy parts of the vasculature and is confirmed by the findings of Noguchi et al (7). For the high-flow dAVF, the arteriovenous transit time was so fast that a simultaneous and identical time course of affluxion artery and draining vein was found. But this finding could be confirmed by conventional angiography showing a simultaneous appearance of arterial feeder and drainage vein.

The in-plane spatial resolution was only slightly improved from 0.97×0.97 mm^2 at the 2D MRA (5, 9) to 0.8×0.8 mm^2 at the herein presented 3D MRA to increase temporal resolution. The section thickness, however, was different: 80 mm for the 2D MRA and 6 mm for the 3D MRA (with 16 sections acquired).

The dominant feeding arteries were sufficiently depicted in the iAVM and the eAVM. The small terminal branch of the affluxion artery of the dAVF could only be suspected. The low diameter of the vessel and the resulting low signal intensity from this feeding artery are accounted as reasons for the missing depiction. The nidus of the eAVM could be clearly depicted, whereas the nidus of the iAVM did not reach sufficient signal intensity to be clearly assessed.

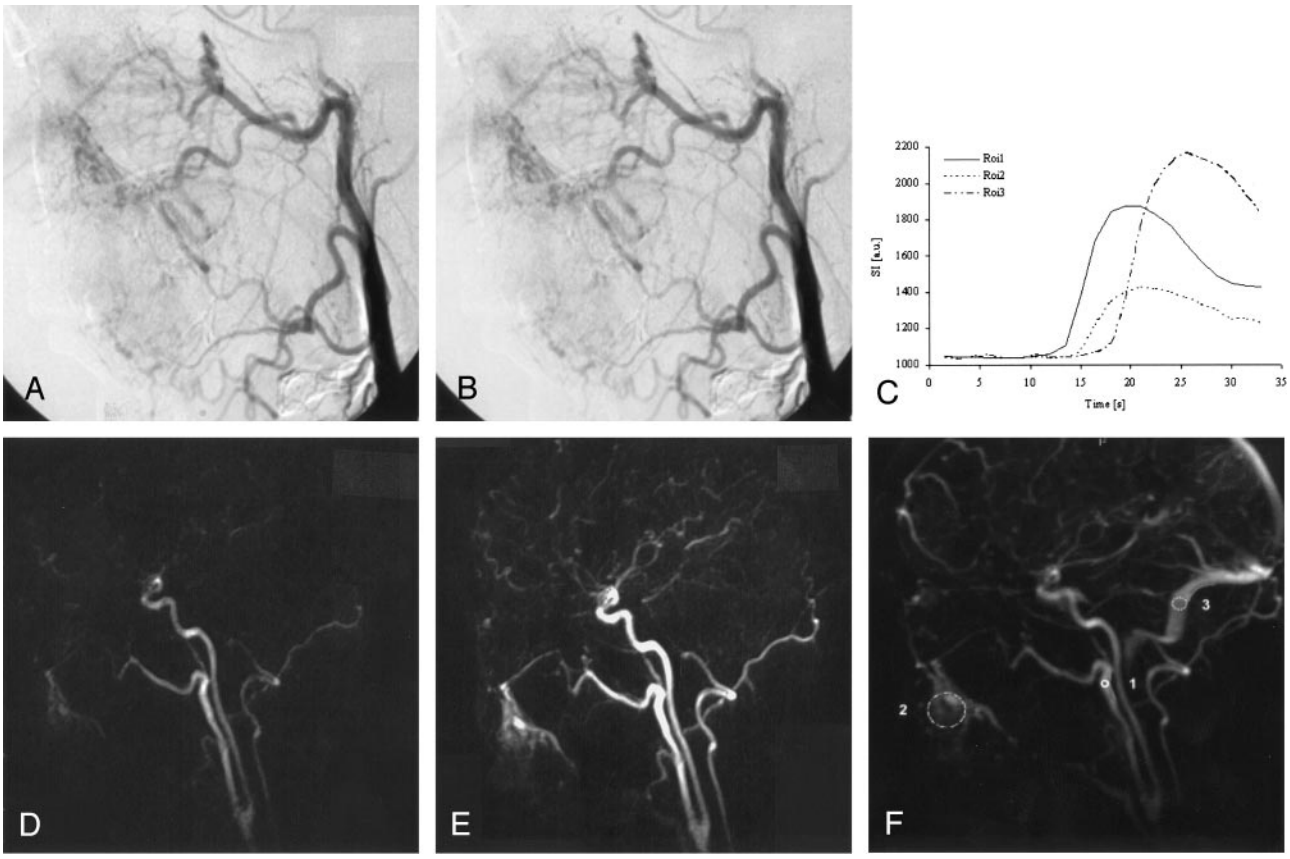

FIG 3. In conventional catheter DSA (*A, B*) a facial AVM is displayed. The infraorbital artery and the facial artery were the arterial feeders; an early draining vein was not present.

Dynamic MRA revealed a facial eAVM consisting of a nidus within the soft tissue below the right mandible. Two feeding arteries, the infraorbital artery and the facial artery were clearly assessed, and the nidus of the eAVM could be clearly depicted in the dynamic 3D MRA (*D, E*). These findings were consistent with the selective, conventional DSA (*A, B*). A region-of-interest analysis of the signal intensity time course (*C, F*) was performed within the external carotid artery (region 1), the nidus (region 2), and the transverse sinus (region 3). The time course of the SI within the region of interest is given in arbitrary units. The difference of contrast arrival time between the external carotid artery and the nidus was 1.5 seconds; the difference of time to peak was 2 seconds. The difference of contrast arrival time between the external carotid artery and the transverse sinus was 4.5 seconds; the difference of time to peak was 7 seconds. The time course of signal intensity showed an intermediate behavior with characteristics of arterial and venous flow. Thus, this example nicely reflects a case of a typical eAVM.

Conclusion

Dynamic 3D MRA combined with parallel imaging could be shown to be advantageous by receiving at temporal resolution of one image per 1.5 seconds which is fast for 3D MRA. Further improvement of temporal resolution may derive from stratified versions of k-space filling into the subsecond domain. For the intracranial and extracranial AVM, the temporal resolution was sufficient by even separating pathologically and normally filled intracranial veins. For the high-flow dural arteriovenous fistula, however, a simultaneous filling of arterial feeder and venous drainage was found by dynamic 3D MRA and conventional angiography.

References

1. Wang Y, Johnston DL, Breen JF, et al. **Dynamic MR digital subtraction angiography using contrast enhancement, fast data acquisition and complex subtraction.** *Magn Reson Med* 1996;36:551–556
2. Hennig J, Scheffler K, Laubenberger J, Strecker R. **Time-resolved projection angiography after bolus injection of contrast agent.** *Magn Reson Med* 1997;37:341–556
3. Strecker R, Scheffler K, Klisch J, et al. **Fast functional MRA using time-resolved projection MR angiography with correlation analysis.** *Magn Reson Med* 2000;43:303–309
4. Aoki S, Yoshikawa T, Hori M, et al. **MR digital subtraction angiography for the assessment of cranial arteriovenous malformations and fistulas.** *AJR Am J Roentgenol* 2000;175:451–453
5. Wetzel SG, Bilecen D, Lyrer P, et al. **Cerebral dural arteriovenous fistulas: detection by dynamic MR projection angiography.** *AJR Am J Roentgenol* 2000;174:1293–1295
6. Coley SC, Romanowski CA, Hodgson TJ, Griffith PD. **Dural arteriovenous fistulae: non-invasive diagnosis with dynamic MR digital subtraction angiography.** *AJNR Am J Neuroradiol* 2002;23:404–407
7. Noguchi K, Melhem ER, Kanazawa T, et al. **Intracranial dural arteriovenous fistulas: evaluation with combined 3D time-of-flight MR angiography and MR digital subtraction angiography.** *AJR Am J Roentgenol* 2004;182:183–190
8. Griffiths PD, Hoggard N, Warren DJ, et al. **Brain arteriovenous malformations: assessment with dynamic MR digital subtraction angiography.** *AJNR Am J Neuroradiol* 2000;21:1892–1899
9. Ziyeh S, Schumacher M, Strecker R, et al. **Head and neck vascular malformations: time-resolved MR projection angiography.** *Neuroradiology* 2003;45:681–686
10. Willinek WA, Gieseke J, von Falkenhausen M, et al. **Sensitivity**

encoding (SENSE) for high spatial resolution time-of-flight MR angiography of the intracranial arteries at 3.0 T. *Rofo Fortschr Geb Rontgenstr Neuen Bildgeb Verfahr* 2004;176:21–26
11. Tsuchiya K, Aoki C, Fujikawa A, Hachiya J. **Three-dimensional MR digital subtraction angiography using parallel imaging and keyhole data sampling in cerebrovascular diseases: initial experience.** *Eur Radiol* 2004;000:00–00
12. Creasy JL, Price RR, Presbrey T, et al. **Gadolinium-enhanced MR angiography.** *Radiology* 1990;175:280–283
13. Griswold MA, Jakob PM, Heidemann RM, et al. **Generalized autocalibrating partially parallel acquisitions (GRAPPA).** *Magn Reson Med* 2002;47:1202–1210
14. Coley SC, Wild JM, Wilkinson ID, Griffiths PD. **Neurovascular MRI with dynamic contrast-enhanced subtraction angiography.** *Neuroradiology* 2003;45:843–850
15. Wetzel S, Meckel S, Bilecen D, et al. **Whole-brain MR-DSA using time-resolved 3D contrast-enhanced MRA and parallel imaging.** *Proc Int Soc Mag Reson Med* 2004;12:415